PHYSICAL REVIEW B

CONDENSED MATTER

THIRD SERIES, VOLUME 37, NUMBER 3 15 JANUARY 1988-II

Density-functional calculations of the electronic properties of metals by the spherical cellular method

Mani Farjam
Department of Physics, University of California, San Diego, La Jolla, California 92093

Herbert B. Shore*
Department of Physics, San Diego State University, San Diego, California 92182
(Received 4 May 1987)

The electronic band-structure calculation of metals using a spherical cellular method is reviewed. The empty-lattice test is applied to the model, and the limitations of the model are discussed. A formula for the pressure in the local-density approximation derived earlier by Janak is shown by a scaling method to be valid for the spherical calculation. First-principles local-density-functional calculations of metals using the spherical cellular method are presented. The band structure of three typical metals, Na, Al, and Cu, are given and compared with the calculations of Moruzzi, Janak, and Williams (MJW). The total energy, equilibrium radius, cohesive energy, bulk modulus, and chemical potential are obtained for H, Li, Na, K, Rb, Mg, Al, and Cu and compared with the results of MJW and experiment. The agreement with MJW is good, particularly for alkali metals, e.g., less than 10% disagreement is found for the cohesive energy of sodium. Our analysis as well as the numerical results suggest that the spherical cellular method works well for *sp* bands, but less well for *d* bands.

I. INTRODUCTION

This paper presents self-consistent local-density-functional calculations of metals, in which the band structure is calculated by a simplified spherical cellular method. The electronic properties of metals, i.e., cohesive energy, band structure, equilibrium density, etc., have been extensively tabulated by Moruzzi, Janak, and Williams (MJW).[1] While this work is quite comprehensive, we have found a need for calculated values of these and related quantities beyond those provided by MJW. For instance, in the calculation of the energy of a positron in a metal at arbitrary volume,[2] one requires the electronic density and, especially, the internal chemical potential at a given crystal volume, generally different from the equilibrium volume at zero temperature. As another example, in the pseudojellium model of the properties of nonuniform metals,[3] e.g., an AB alloy or a bimetallic interface, one requires the cohesive energy and the internal chemical potential as a functions of average electronic and ionic densities, where due to charge transfer the individual cells are not necessarily neutral.

It is of course not feasible to tabulate such quantities for every conceivable range of parameters; rather, what is needed is a relatively simple method for calculating these quantities with reasonable accuracy and computational efficiency. The purpose of our study is, therefore, not to provide an alternative method for obtaining the results already calculated by MJW, but to enable us to extend their results to a wider range of conditions. A main goal of this paper is to study the reliability of the spherical cellular method and to examine the conditions under which it can be expected to produce reasonable numerical results.

The cellular method, of which we use a simplified version, was used by Wigner and Seitz[4] to calculate the $k=0$ wave function of the $3s$ conduction band of sodium. There have been continued attempts to make the cellular method more practical and accurate,[5] but since we are interested in a simplified version we only mention two important improvements. One is the use of symmetry for a more efficient expansion of the wave function,[6] and the other is the application of variational principles to the fitting of the boundary conditions over the surface of the cell.[7]

In the spherical cellular model (SCM) we replace the Wigner-Seitz polyhedron by a sphere of equivalent volume and define a set of boundary conditions on the surface of the sphere to simulate the Bloch conditions.

Together with a central potential, we can expand the wave functions in the spherical harmonics and easily solve this simplified model. A drawback of this model is that periodicity is lost, because spheres cannot be space-filling cells, neither can the band structure thus obtained be periodic in a reciprocal lattice. However, if the position and the width of the bands are well reproduced, the model can be very useful for certain applications. We also note that the differences in the total energy of metals calculated for different crystal structures, e.g., bcc and fcc, tend to be a small fraction of their cohesive energy. Thus one can hope that SCM, which represents an "average" over different structures, should lead to a total energy in reasonable agreement with the full lattice calculations.

The formalism of the SCM was developed by Brooks[8] who used it in the calculation of the cohesive energy of the alkali metals. It has been generalized by Gandel'man[9] and by Berggren and Fröman[10] to include higher bands and it has been used in the study of metals under compression.[11] Density-functional calculations based on spherical cellular methods have been performed by Tong,[12] who calculated the cohesive energy of sodium, and by Zaremba who applied the method to the heat of formation of alloys.[13] In these applications only s-wave derived bands were considered.

In Sec. II we review the formalism of the SCM and describe the procedure for self-consistent calculations, and also rederive a formula for the pressure of the cell, using the scaling method. In Sec. III we analyze the model by making use of the empty lattice test and the symmetries of the wave functions. In Sec. IV we present the results of numerical calculations of several metals and compare them with other calculations and with experimental results. Section V contains a summary and discussions.

II. THEORY

A. Spherical cellular method and self-consistent calculations

The formalism of the SCM reviewed in this section is similar to the derivations of Refs. 9 and 10, though it was developed independently. We shall use atomic units for length and Rydbergs for energy. It is convenient to write the boundary conditions on the spherical cell with the phase factor $\exp(2ikR_s\cos\theta)$ distributed on both sides of the equation:[8]

$$e^{-ikR_s\cos\theta}\Psi_k(r,\theta,\phi)=e^{ikR_s\cos\theta}\Psi_k(r,\pi-\theta,\phi+\pi)\ , \tag{1a}$$

$$e^{-ikR_s\cos\theta}\frac{\partial}{\partial r}\Psi_k(r,\theta,\phi)\Big|_{r=R_S}=-e^{ikR_s\cos\theta}\frac{\partial}{\partial r}\Psi_k(r,\pi-\theta,\phi+\pi)\Big|_{r=R_S}\ , \tag{1b}$$

where R_s is the radius of the spherical cell. We point out a difference in the way the boundary conditions are fitted on a Wigner-Seitz polyhedron as compared to fitting them on a sphere. In a polyhedron the boundary conditions are applied to a pair of points $\mathbf{r}$ and $\mathbf{r}'$ on opposite faces related by reflection in a plane parallel to the faces, whereas Eqs. (1) are applied to the pair of points $\mathbf{r}$ and $-\mathbf{r}$ related by inversion (see Fig. 1). Obviously, the difference will be small if the polyhedron is nearly spherical and its faces are small. We shall return to this point in the discussion of the empty lattice test.

It is important that the Hamiltonian is Hermitian with respect to the space of the functions satisfying Eqs. (1). To check this we consider the kinetic energy of a wave function that satisfies these boundary conditions:

$$\begin{aligned}\int\Psi^*(-\nabla^2)\Psi\,d\mathbf{r}&=-\int_V\nabla\cdot(\Psi^*\nabla\Psi)d\mathbf{r}\\&\quad+\int_V\nabla\Psi^*\cdot\nabla\Psi\,d\mathbf{r}\\&=\int_S\Psi^*\nabla\Psi\cdot d\mathbf{S}+\int_V\nabla\Psi^*\cdot\nabla\Psi\,d\mathbf{r}\ .\end{aligned} \tag{2}$$

It would be enough to show that the surface integral is zero. From Eq. (1) it follows that

$$\Psi^*\frac{\partial\Psi(\mathbf{r})}{\partial r}\Big|_{r=R_S}=-\Psi^*\frac{\partial\Psi(-\mathbf{r})}{\partial r}\Big|_{r=R_S}\ , \tag{3}$$

and this makes the surface integral zero, because contributions from $\mathbf{r}$ and $-\mathbf{r}$ cancel each other for each $\mathbf{r}$ on the surface.

We note that an axis of symmetry along $\mathbf{k}$ is implied by Eq. (1), and that for zero $\mathbf{k}$, spherical symmetry is restored. The states at $\mathbf{k}=0$ are, therefore $(2l+1)$-fold degenerate and can be labeled by the l and m quantum numbers. For states of even and odd parity under inversion, corresponding to even and odd l, the boundary conditions simplify to $\Psi'_{k=0}(R_S)=0$ and $\Psi_{k=0}(R_S)=0$, respectively. For $\mathbf{k}\neq0$, the eigenstates become admixtures of different l; however, m remains a good quantum number, with bands of given $|m|$ remaining doubly degenerate for $|m|>0$. Assuming the effective potential has spherical symmetry, we can expand the wave functions in spherical harmonics

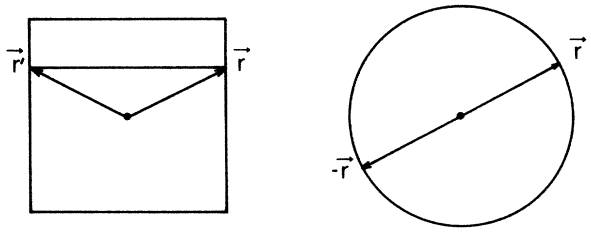

FIG. 1. The boundary conditions are applied to a pair of points $\mathbf{r}$ and $-\mathbf{r}$, (a) in a Wigner-Seitz polyhedron and (b) in its spherical cell equivalent.

$$\Psi_k^m(\mathbf{r})=\sum_{l=m}^{\infty} i^l A_{lm} Y_l^m(\theta,\phi) R_l(E_k,r) , \tag{4}$$

where $u_l(r)=rR_l(r)$ satisfies the radial equation

$$\frac{d^2u_l}{dr^2}+[E-V(r)-l(l+1)]u_l=0 . \tag{5}$$

The energy E_k depends only on the magnitude of $\mathbf{k}$ since there is no preferred direction for $\mathbf{k}$.

If we substitute Eq. (4) into Eq. (1), multiply by $Y_l^{m*}(\theta,\phi)$, and integrate over angle, we obtain

$$\sum_{l=m}^{\infty} i^l B_{lm} R_l'(E_k,R_S) I_{lL}^m(kR_S)=0, \quad \text{even } L \tag{6a}$$

$$\sum_{l=m}^{\infty} i^l B_{lm} R_l(E_k,R_S) I_{lL}^m(kR_S)=0, \quad \text{odd } L , \tag{6b}$$

where

$$I_{lL}^m(kR_S)=\int \frac{d\Omega}{2\pi} e^{-ikR_S\cos\theta} P_l^m(\cos\theta) P_L^m(\cos\theta) , \tag{7}$$

and

$$B_{lm}=\left[\frac{2l+1}{4\pi}\frac{(l-m)!}{(l+m)!}\right]^{1/2} A_{lm} . \tag{8}$$

The matrix I_{lL}^m is most conveniently calculated by direct quadrature. Expanding the exponential plane wave term in spherical Bessel functions as in Brooks[8] yields a less efficient expression for numerical evaluation. The band energies are found for given k and m using Eqs. (6) by locating the zero of the determinant of the coefficients that multiply the B_{lm}, using an interpolation method.

The effective potential $V(r)$ in Eq. (5), as obtained from a self-consistent all-electron density-functional calculation,[14] is given by

$$V(\mathbf{r})=-\frac{2Z}{r}+2\int \frac{\rho(\mathbf{r}')}{|\mathbf{r}-\mathbf{r}'|}d\mathbf{r}'+\mu_{xc}(\mathbf{r}) , \tag{9}$$

where the first two terms are the electrostatic potential and $\mu_{xc}(\mathbf{r})$ is the effective exchange-correlation potential. The electron density for band m is given by

$$\rho^m(\mathbf{r})=2\sum_{k(E_k<E_F)} |\Psi_k^m(\mathbf{r})|^2 . \tag{10}$$

We restricted the summation to a spherical zone having the same volume as the first Brillouin zone. For states sufficiently far below E_F, i.e., core levels, Ψ_k can be replaced by $\Psi_{k=0}$. The total density is the sum of all band and core densities. The Fermi energy, and hence the Fermi momentum, is in general determined by the total number of electrons. The Fermi surface is spherical in the SCM, so for metals with only a single band present at the Fermi level, k_F will be given by $(9\pi/4)^{1/3}1/R_S$ for a half-filled band or $(9\pi/2)^{1/3}1/R_S$ for a completely filled band. Equation (10) implies that the density and, consequently, the potential is spherically symmetric.

We used the local-density approximation of the exchange-correlation potential

$$\mu_{xc}=\frac{d}{d\rho}[\rho\epsilon_{xc}(\rho)]\bigg|_{\rho=\rho(r)} . \tag{11}$$

In order to make our results as comparable as possible with those of MJW, we use the Hedin-Lundqvist parametrization for ϵ_{xc}:[15]

$$\epsilon_{xc}=-\frac{0.916}{r_S}-0.045G(x) , \tag{12}$$

with $x=r_S/21$. Here r_S is the radius parameter related to density by $\rho^{-1}=4\pi r_S^3/3$, and

$$G(x)=(1+x^3)\ln(1+1/x)-x^2+x/2-\tfrac{1}{3} . \tag{13}$$

Numerical solutions for energy eigenvalues, ϵ_k, and eigenfunctions, in terms of the A_{lm}, are obtained from Eq. (6). A total of 8 to 12 values of k were calculated for each band. Termination of the infinite sums at $l_{max}=6$ was found to be adequate, i.e., increasing l_{max} did not change the results significantly. The radial functions R_l were obtained from a numerical solution of the radial equation. In order to obtain a starting potential for the band-structure calculation, we simply used the potential of the bare nucleus, and performed several iterations with $k=0$ boundary conditions for all states. Self-consistency was achieved in about a total of 20 iterations.

B. Total energy and pressure

The total energy is

$$E=T+U+E_{xc} , \tag{14}$$

where the kinetic energy is given by

$$T=\sum_i \int \Psi^* i(-\nabla^2)\Psi_i d\mathbf{r}=\sum_i \epsilon_i-\int \rho(\mathbf{r})V(\mathbf{r})d\mathbf{r} , \tag{15}$$

the sum extending over all the occupied states, and the potential energy is given by

$$U=\int \rho(\mathbf{r})\left[\frac{-2Z}{r}\right]d\mathbf{r}+\int\int \frac{\rho(\mathbf{r})\rho(\mathbf{r}')}{|\mathbf{r}-\mathbf{r}'|}d\mathbf{r}\,d\mathbf{r}' . \tag{16}$$

The last term in Eq. (14) is the exchange-correlation energy given in the local-density approximation by

$$E_{xc}=\int \rho(\mathbf{r})\epsilon_{xc}(\rho(\mathbf{r}))d\mathbf{r} , \tag{17}$$

with ϵ_{xc} given by Eq. (12). The integrals are carried out within the unit cell, $r<R_S$; in the SCM there are no corrections due to intercell interactions.

A numerical calculation of the pressure, requiring several calculations of energy at various values of R_S, can be based on

$$P=-\frac{dE}{dV}=-\frac{1}{4\pi R_S^2}\frac{dE}{dR_S} . \tag{18}$$

It is, however, more useful to have a formula for the pressure requiring a single calculation at a particular R_S. Such a formula was obtained by Janak[6] by considering

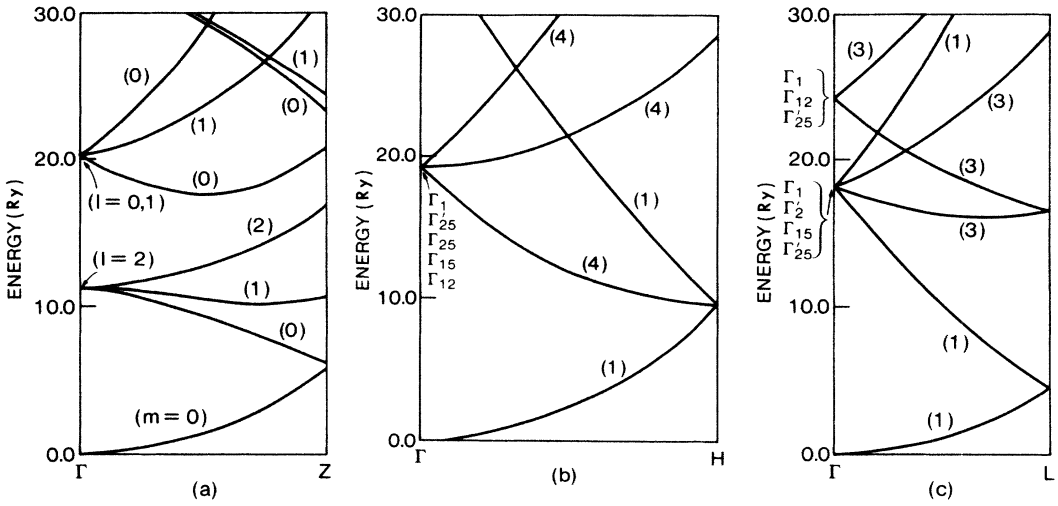

FIG. 2. Comparison of the empty lattice band structures for (a) a spherical cell and, (b) and (c), special symmetry directions of bcc and fcc lattices, respectively. The cells are adjusted to have the same volume, so that with $R_s=1$, $a_{bcc}=(8\pi/3)^{1/3}$ and $a_{fcc}=(16\pi/3)^{1/3}$. The Γ point of each band is labeled, in (a), by the angular momentum quantum number l and, in (b) and (c), by their representations of the cubic point group. The bands in (a) are specified by the m quantum number; for zero m values they are nondegenerate and otherwise doubly degenerate. The numbers next to the bands in (b) and (c) are the degeneracies of the bands. In all three cases the first band is given by $\epsilon=k^2$.

the expectation value of the $\mathbf{r}\cdot\nabla$ operator. This approach involves the evaluation of surface integrals of the polyhedral cell, making it difficult to verify with the boundary conditions of Eq. (1). We derive the same formula by an approach used by Slater[17] to derive the virial theorem and pressure equation in the $X\alpha$ approximation.

In this approach one applies the variational principle to a particular set of scaled trial wave functions. To obtain this set, we imagine solving the same Hamiltonian but for a cell of radius λR_S, calling the wave functions $\phi_i(\mathbf{r},\lambda R_S)$. The norm preserving scaled wave functions

$$\Psi_i(\mathbf{r})=\lambda^{3/2}\phi_i(\lambda\mathbf{r},\lambda R_s) \tag{19}$$

can then be used as trial wave functions for the original problem. The corresponding densities are related by

$$\rho(\mathbf{r})=\lambda^3 w(\lambda\mathbf{r},\lambda R_S)\ , \tag{20}$$

where $\rho(\mathbf{r})=\sum_i |\Psi_i(\mathbf{r})|^2$ and $w(\mathbf{r})=\sum_i |\phi_i(\mathbf{r})|^2$, with the sums extending over all the occupied states. Substituting these forms for the wave function and the density in Eqs. (15) and (16) for the kinetic and potential energy, it is obvious that

$$T=\lambda^2 T(\lambda R_S) \tag{21}$$

and

$$U=\lambda U(\lambda R_S)\ , \tag{22}$$

where $T(\lambda R_S)$ and $U(\lambda R_S)$ are the kinetic and potential energies of the system of radius λR_S. So far this is following Slater's derivation, but the exchange-correlation energy, not necessarily being a homogeneous function of the coordinates, scales differently:

$$\begin{aligned} E_{xc} &= \int \rho(\mathbf{r})\epsilon_{xc}(\rho(\mathbf{r}))d\mathbf{r} \\ &= \int w(\lambda\mathbf{r})\epsilon_{xc}(\lambda^3 w(\lambda\mathbf{r}))d(\lambda^3\mathbf{r}) \\ &= \int w(r)\epsilon_{xc}(\lambda^3 w(\mathbf{r}))d\mathbf{r}\ . \end{aligned} \tag{23}$$

Since the Kohn-Sham wave functions for the $\lambda=1$ problem exactly minimize the energy functional of Eq. (14), a modified virial theorem can now be found by applying the variational principle, $dE/d\lambda\,|_{\lambda=1}=0$,

TABLE I. Γ-point energies and corresponding group representations for SCM, bcc, and fcc cells of equal volume. The numbers in parentheses are the degeneracies of the levels. The entries of each row are selected according to the correspondence between the representations as given by Eq. (29).

SCM		bcc		fcc	
0.0	$D_0(1)$	0.0	$\Gamma_1(1)$	0.0	$\Gamma_1(1)$
11.7	$D_2(5)$	19.14	$\Gamma_{12}(2)$	18.09	$\Gamma'_{25}(3)$
			$\Gamma'_{25}(3)$	24.12	$\Gamma_{12}(2)$
20.19	$D_0(1)$	19.14	$\Gamma_1(1)$	18.09	$\Gamma_1(1)$
	$D_1(3)$		$\Gamma_{15}(3)$		$\Gamma_{15}(3)$

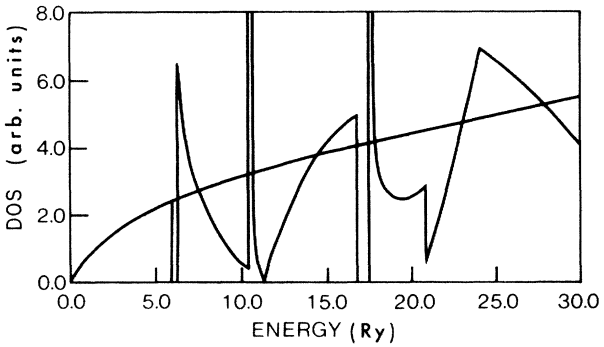

FIG. 3. Empty lattice DOS obtained by the spherical cellular method. Also shown is the exact free particle DOS $\sim \epsilon^{1/2}$. The section of the first band, that is, $\epsilon < (9\pi/2)^{2/3}$, is exact, but the sections of the higher bands are only on rough agreement with the exact result. The SCM has introduced artificial gaps and infinities in the density of states.

$$R_S \frac{dE}{dR_S} = -2T - U - \int \rho(\mathbf{r}) \left[\lambda \frac{\partial \epsilon_{xc}(\lambda^3 \rho(\mathbf{r}))}{\partial \lambda} \right]_{\lambda=1} d\mathbf{r} \ . \tag{24}$$

In the last term we have

$$\lambda \frac{\partial \epsilon_{xc}(\lambda^3 \rho)}{\partial \lambda} = 3\lambda^3 \rho \frac{d\epsilon_{xc}}{d\rho} \ . \tag{25}$$

Together with the LDA result, $\mu_{xc} = \rho \frac{d\epsilon_{xc}}{d\rho} + \epsilon_{xc}$, and Eq. (25) we can rewrite Eq. (24) as

$$R_s \frac{dE}{dR_S} = -2T - U + 3 \int \rho(\epsilon_{xc} - \mu_{xc}) d\mathbf{r} \ . \tag{26}$$

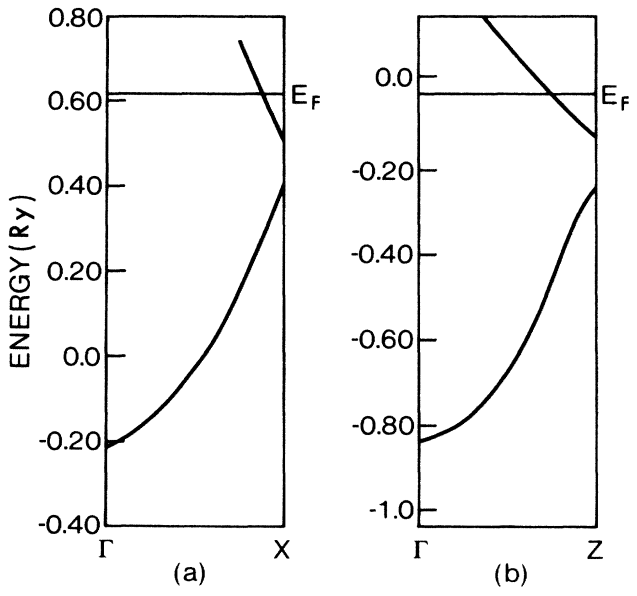

FIG. 5. Same as Fig. 4, but for aluminum. The overall agreement is quite good, although the second band is flatter in the SCM calculation.

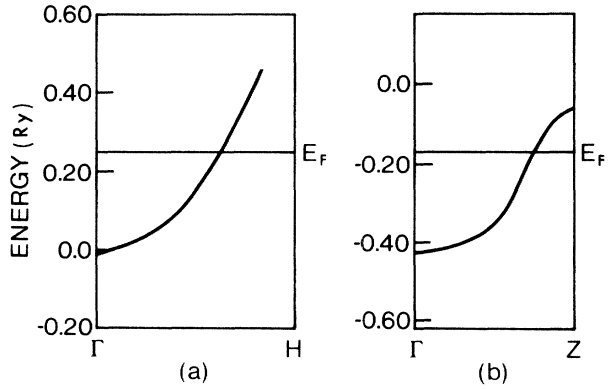

FIG. 4. Band structure of sodium, (a) from MJW and (b) calculated by the SCM, for an r_S derived from the tabulated lattice constants of MJW. The Fermi energy, for both cases, is drawn at the same level for comparison. The zero in (a) refers to the muffin-tin potential, but in (b) it refers to the electrostatic potential. Below E_F, the bands are in excellent agreement.

From Eq. (18), with $v = 4\pi R_S^3/3$ volume of the cell, it follows that

$$3Pv = 2T + U - 3 \int \rho(\epsilon_{xc} - \mu_{xc}) d\mathbf{r} \ . \tag{27}$$

This is the formula obtained by Janak. It will be used in the following to provide a check for the numerical accuracy of our calculations, since P as calculated by Eq. (27) or Eq. (18) must agree.

III. EMPTY LATTICE TEST

Free electrons with wave functions $\Psi_{\mathbf{k}} = \exp(i\mathbf{k}\cdot\mathbf{r})$ and energy $\epsilon = k^2$ provide a simple test of a band-structure

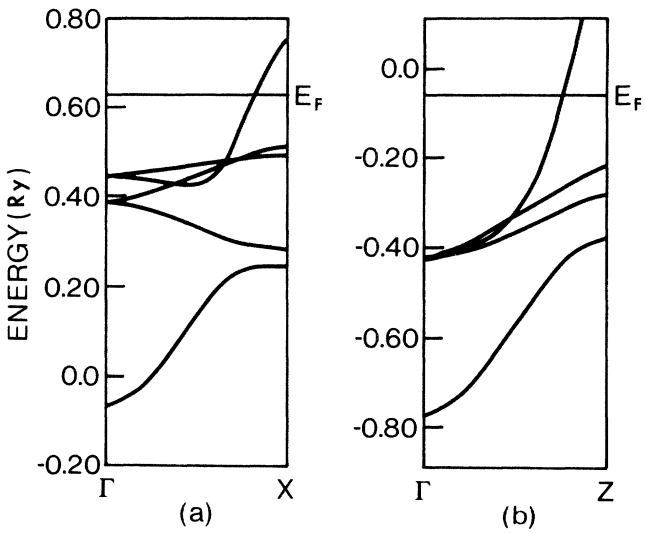

FIG. 6. Same as Fig. 4, but for copper. Hybridization between s and d bands can be seen in both cases. In the SCM, hybridization is the result of the fact that the $m = 0$ levels cannot cross. The bandwidths, below E_F, are quite similar, and the d bands are in rough agreement, in both location and bandwidth.

TABLE II. Energies of special points in Rydbergs (relative to Fermi energy). Degeneracy of a point is given in parentheses. The radii are derived from the tabulated lattice constants of MJW. The spherical cell radius is $r_s n^{1/3}$ where n is the valency.

		Zone center		Zone edge	
		MJW	This work	MJW	This work
Metal	r_S		Γ point	X point	Z point
Na	3.79	−0.255	−0.254		0.129
Al				−0.208	−0.202
	2.06	−0.823	−0.818	−0.131	
					−0.085
				−0.387	
Cu		−0.692	−0.713	−0.344	−0.314
		−0.238(3)		−0.234	−0.158(2)
	2.64				
			−0.364(5)	−0.117(2)	−0.221(2)
		−0.177(2)			
				0.120	0.225

calculation. plane waves are seen to satisfy the boundary conditions of the spherical cellular model, with $\epsilon=k^2$, and are exact solutions. However, the band structure obtained from SCM is not periodic in $\mathbf{k}$ space, and its properties have to be investigated in the reduced zone. We restrict k to a sphere of the same volume as the first Brillouin zone giving a radius of $k_Z=(9\pi/2)^{1/3}1/R_S$, satisfying

$$\frac{4\pi}{3}R_s^3\frac{4\pi}{3}k_Z^3=(2\pi)^3 . \tag{28}$$

In Fig. 2 are shown the empty lattice band structures of the SCM, fcc and bcc lattices for special directions of high symmetry.[18] We point out that in the SCM the band structure does not depend on the direction of $\mathbf{k}$, whereas in the real lattices it does. The lowest band, which does not depend on the structure, is given correctly by SCM as $\epsilon=k^2$, but the higher bands depend on the structure and cannot be compared. A direct quantitative comparison, except a semiquantitative one at $\mathbf{k}=\mathbf{0}$, is not useful, but the density of states, being a sum over all directions, can be used for an indirect comparison.

We first compare the $\mathbf{k}=\mathbf{0}$ levels of SCM, bcc and fcc, including both the values and symmetries. In the SCM, the atomic levels s,p,d, etc. are shifted but not split; for free particles, the s and p levels, except for the lowest band, turn out to be degenerate.

The angular momentum representations, D_l, are reducible in terms of the representations of the octahedral group O_h:[18]

$$\begin{aligned} D_0&=\Gamma_1 , \\ D_1&=\Gamma_{15} , \\ D_2&=\Gamma_{12}+\Gamma'_{25} . \end{aligned} \tag{29}$$

In Table I we compare a few levels at $k=0$ based on their symmetries. The s and p levels compare well, but the d level is considerably lower than the corresponding levels in bcc and fcc. This disagreement is a consequence of the point we made in Fig. 1, together with the different boundary conditions for even and odd parity. We recall that for $k=0$ the boundary condition for even parity is zero slope and for odd parity zero value. The zero-slope condition requires less curvature of the wave function than zero value condition, and thus will give a lower energy. (An exponential atomiclike boundary condition will give something in between.) In a spherical cell, where parity refers to inversion, one or the other boundary condition is satisfied exclusively over the entire

TABLE III. Total energies in Rydbergs of several metals at the r_S used by MJW.

Metal	r_S	E MJW	E Present work
H	1.68	−1.076	−1.081
Li	3.16	−14.832	−14.839
Na	3.79	−322.985	−322.991
K	4.65	−1196.448	−1196.456
Rb	5.03	−5872.525	−5872.544
Mg	2.60	−398.401	−398.421
Al	2.06	−482.922	−482.912
Cu	2.64	−3275.768	−3275.803

TABLE IV. Equilibrium values of r_S compared with experimental values and MJW. Spherical radius R_s is related to the radius parameter r_S by $R_s=r_s n^{1/3}$ where n is the valency.

Metal	r_s Experimental	r_s MJW	r_S Present work
Li	3.25	3.16	3.07
Na	3.93	3.79	3.69
K	4.86	4.65	4.47
Rb	5.20	5.03	4.65
Mg	2.65	2.60	2.52
Al	2.07	2.06	2.19
Cu	2.67	2.64	2.60

TABLE V. Cohesive energy in Rydbergs and bulk modulus in Mbars.

Metal	E[a] Experiment	E MJW	E This work	B^* Experiment	B MJW	B This work
Li	0.120	0.121	0.131	0.116	0.15	0.16
Na	0.082	0.082	0.089	0.068	0.09	0.09
K	0.069	0.066	0.075	0.032	0.04	0.04
Rb	0.063	0.047	0.071	0.031	0.03	0.03
Mg	0.111	0.124	0.149	0.354	0.41	0.48
Al	0.249	0.282	0.289	0.722	0.80	1.20
Cu	0.257	0.301	0.346	1.37	1.55	1.80

[a]Reference 19.

cell surface, but in a Wigner-Seitz polyhedron parity refers to reflection and a mixture of zero-slope and zero-value boundary conditions may have to be satisfied. The eigenstates of angular momentum with nonzero l, having nodal surfaces that pass through the origin, are examples of this point, whereas the $l=0$ state has even parity under both inversion and reflection. From this we conclude that we can expect the SCM to work well for s states, but less well for p and d states.

We now turn to the other test of the model by the density of states defined by

$$N(\epsilon)=\frac{1}{4\pi^3}\int\frac{dS}{|\nabla_k\epsilon|}\ , \tag{30}$$

where the integral is over a constant energy surface. This is simple to calculate for spherical energy surfaces, which is the case in the SCM for free particles as well as particles moving in a potential. The exact result for free particles is given by $N(\epsilon)=\epsilon^{1/2}/2\pi^2$. The empty lattice DOS by the SCM is shown in Fig. 3, which, except for the first band, shows considerable local deviation.

We conclude this section by saying that for alkali metals, with a nearly free-electron spectrum and a single valence electron, we can expect the SCM to work well. As more valence electrons are added in aluminum, or d bands are filled in the transition and noble metals, the results become less reliable. We further investigate this question in the next section by presenting the results of numerical calculations of several metals.

IV. NUMERICAL CALCULATIONS

In this section we will make extensive use of the tabulated results of MJW to compare with our calculations. They use the Korringa-Kohn-Rostoker (KKR) method and the muffin-tin approximation of the potential, but, otherwise, use the local-density approximation with the same form of exchange-correlation energy[15] as this work.

In Figs. 4–6 we compare the band-structure calculations of three typical metals, sodium, aluminum, and copper with those of MJW. In Table II we list the band energies at special symmetry points. The band structure of sodium below the Fermi energy is similar to that of MJW, as can be seen from Fig. 4 and Table II. The similarity between our calculation and MJW is also evident for aluminum in Fig. 5. For all three metals, the overall bandwidths (below the Fermi energy) are in good agreement. For copper, hybridization between s and d bands can be seen in both Figs. 6(a) and 6(b). In the SCM calculation, hybridization results because the $m=0$ levels cannot cross. The s bands are in good agreement, but the d bands are only in rough agreement in location and bandwidth.

In Table III we compare the total energies for several metals with the results of MJW. For the alkali metals we find that several of the topmost core states have large enough amplitude at R_S that they must be treated as bands. This is made evident by applying zero-value or zero-slope boundary conditions to the particular states, and using the fact that the zero-value condition always increases the pressure, while the zero-slope condition always decreases the pressure. If the difference in pressure between the two types of boundary conditions is significant, then that state must be treated as a band. The agreement with MJW for the alkali metals is good; the discrepancy is in part due to the core states, because they have a more complicated band structure.

Our equilibrium values of r_S, given in Table IV, are, except for Al, smaller than those of MJW which are in turn smaller than experimental values. Again, for alkali metals, since the minimum of energy versus r_s is very shallow, the equilibrium r_s depends on the treatment of the core levels, and we could have expected better agreement with MJW had the core levels been less important.

The results of the calculations for cohesive energy and bulk modulus are given in Table V and compared with experimental results[19] and MJW. Our results for cohensive energies are larger, by 10 to 30%, than the results of MJW, the best agreement being for the alkali metals and the worst for copper. Both theoretical calculations tend to give higher cohesive energy than experiment, but the agreement is still quite good. For lithium and sodium MJW reproduce the experimental values and our results are only 8% larger. We note that the cohesive energy is the difference between two large numbers: The total energy of Table III and the energy of separated atoms. Thus we regard the agreement obtained as impressive. Our results for the bulk moduli are virtually the same as MJW for alkali metals, but as much as 50% higher for aluminum and about 20% higher for magnesium and copper. Both theoretical calculations tend to give higher values than experiment.

The values of the chemical potential at two different volumes are given in Table VI. The chemical potential

at zero temperature is the Fermi level, measured relative to the zero of the electrostatic potential. For a neutral system the electrostatic potential becomes zero on the surface of the spherical cell. Our values of μ are compared with the theoretical values of Weinert and Watson[20] who based their calculations of the chemical potential on the data MJW, who tabulate the Fermi energy only relative to the muffin-tin zero. Our values at the equilibrium volume of MJW are within 0.2 eV of Weinert and Watson. We also point out the strong dependence of the chemical potential on the cell volume. The chemical potential generally increases in magnitude with r_s and the increase is of the order of 0.1 eV per 0.1 units increase in r_s for the alkali metals and closer to 1 eV for aluminum and copper for the same increase in r_s, all near the equilibrium r_s. We therefore expect μ calculated at the experimental r_s, rather than the equilibrium r_s, to be the reliable value.

TABLE VI. Internal chemical potential in eV.

Metal	μ^a	μ^b	μ^c
Li	−2.2	−2.4	−2.2
Na	−2.2	−2.3	−2.1
K	−2.1	−2.2	−2.0
Rb	−2.1	−2.2	−1.8
Mg	−1.4	−1.9	−1.5
Al	−0.2	−0.3	−1.6
Cu	−0.8	−0.8	−0.4

[a]Reference 20.
[b]Calculated at r_S values of MJW, given in Table IV.
[c]Calculated at equilibrium r_S values, also given in Table IV.

V. SUMMARY

We have investigated the use of the spherical cellular method combined with a self-consistent density-functional calculation in the calculation of the band structure and bulk properties of metals. From the empty lattice test we found that the band structure for *sp* bands can be quite accurate. By comparing with the band structure of three typical metals, Na, Al, and Cu, this was confirmed for real metals as well. For bands that develop from the *p* and *d* atomic states we found only rough agreement with more accurate calculations. We also compared the numerical results for the bulk properties, with calculations of MJW and experiment. For cohesive energy we found good agreement with MJW and experiment, and could explain the discrepancies based on the analyses of the method. The results for equilibrium radii were usually smaller by a few tenths of atomic units than the results of MJW, and this was attributed in part to the effect of the core states. The bulk moduli of alkali metals were in good agreement with the results of MJW, but for Al, Mg, and Cu the agreement was only fair. The results for the chemical potential were in good agreement with the calculation of Weinert and Watson. We determined the chemical potential at two different sets of r_S, and found that it varies sensitively with this parameter. In fact, it is useful to be able to calculate the chemical potential as a function of volume, or other parameters, for applications to nonuniform systems.[3] In conclusion, we have shown that the SCM can be a relatively convenient way of calculating bulk properties of metals, and have also analyzed its applicability and limitations.

ACKNOWLEDGMENT

This work was supported in part by the National Science Foundation under Grant No. DMR-82-17708.

*Present address: Division of Materials Research, National Science Foundation, Washington D.C. 20550

[1]V. L. Moruzzi, J. F. Janak, and A. R. Williams, *Calculated Electronic Properties of Metals* (Pergamon, New York, 1978).
[2]M. Farjam and H. B. Shore, Phys. Rev. B **36**, 5089 (1987).
[3]C. A. Utreras and H. B. Shore, Phys. Rev. Lett. **53**, 2335 (1984).
[4]E. P. Wigner and F. Seitz, Phys. Rev. **43**, 804 (1933); **46**, 509 (1934).
[5]A. C. Ferraz, E. K. Takahashi, and J. R. Leite, Phys. Rev. B **26**, 690 (1982).
[6]F. C. Von Der Lage and H. A. Bethe, Phys. Rev. **71**, 612 (1947).
[7]W. Kohn, Phys. Rev. **87**, 472 (1952).
[8]H. Brooks, Nuovo Cimento Suppl. **7**, 165 (1958).
[9]G. M. Gandel'man, Zh. Eksp. Teor. Fiz. **43**, 131 (1962) [Sov. Phys.—JETP **16**, 94 (1963)].
[10]K.F. Berggren and A. Fröman, Ark. Fys. **39**, 355 (1969).
[11]G. M. Gandel'man, Zh. Eksp. Teor. Fiz. **51**, 147 (966) [Sov. Phys.—JETP **24**, 99 (1967)]; L. V. Al'tshuler, A. I. Voropinov, G. M. Gandel'man, N. A. Dmitriyev, and V. G. Podval'nyy, Phys. Met. Metallogr. (USSR) **51**, 61 (1981).
[12]B. Y. Tong, Phys. Rev. B **6**, 1189 (1972).
[13]E. Zaremba, Solid State Commun. **44**, 931 (1982).
[14]W. Kohn and L. J. Sham, Phys. Rev. **140**, A1133 (1965).
[15]L. Hedin and B. I. Lundqvist, J. Phys. C **4**, 2064 (1971).
[16]J. F. Janak, Phys. Rev. B **9**, 3985 (1974).
[17]J. C. Slater, *The Self-Consistent Theory of Molecules and Solids,* Vol. 4 of *Quantum Theory of Molecules and Solids* (McGraw-Hill, New York, 1974), p. 289.
[18]C. Kittel, *Quantum Theory of Solids* (Wiley, New York, 1963), p. 206.
[19]C. Kittel, *Introduction to Solid State Physics,* 6th ed. (Wiley, New York, 1986), pp. 55–57 and references therein.
[20]M. Weinert and R. E. Watson, Phys. Rev. B **29**, 3001 (1984).